

1 **Rapid genotyping of tilapia lake virus (TiLV) using Nanopore sequencing**

2
3 Jerome Delamare-Deboutteville^{1*}, Suwimon Taengphu², Han Ming Gan³, Pattanapon
4 Kayansamruaj⁴, Partho Pratim Debnath⁵, Andrew Barnes⁶, Shaun Wilkinson^{7,8}, Minami
5 Kawasaki⁶, Chadag Vishnumurthy Mohan¹, Saengchan Senapin^{2,9}, Ha Thanh Dong^{10*}

6
7 ¹WorldFish, Penang, Malaysia

8 ²Fish Health Platform, Center of Excellence for Shrimp Molecular Biology and Biotechnology (Centex
9 Shrimp), Faculty of Science, Mahidol University, Bangkok, Thailand

10 ³GeneSEQ Sdn Bhd, Rawang 48300, Selangor, Malaysia

11 ⁴Center of Excellence in Aquatic Animal Health Management, Faculty of Fisheries, Kasetsart University,
12 Bangkok, Thailand

13 ⁵WorldFish, Khulna, Bangladesh

14 ⁶The University of Queensland, School of Biological Sciences and Centre for Marine Science, Brisbane,
15 Queensland, 4072, Australia

16 ⁷School of Biological Sciences, Victoria University of Wellington, Wellington, New Zealand,

17 ⁸Wilderlab NZ Ltd., Wellington, New Zealand

18 ⁹National Center for Genetic Engineering and Biotechnology (BIOTEC), National Science and
19 Technology Development Agency (NSTDA), Pathum Thani, Thailand

20 ¹⁰Faculty of Science and Technology, Suan Sunandha Rajabhat University, Bangkok, Thailand

21
22 *Corresponding authors:

23 J. Delamare-Deboutteville, j.delamare@cgiar.org

24 H.T. Dong, hathanh.do@ssru.ac.th

25
26

27

28

29

30

31

32

33

34

35

36

37

38

39

40

41

42

43

44 **Acknowledgments**

45 This work was undertaken as part of the CGIAR Research Program on Fish Agri-Food Systems
46 (FISH) led by WorldFish, and the CGIAR Big Data Platform Inspire Challenge 2019 led by
47 CIAT and IFPRI. These programs are supported by contributors to the CGIAR Trust Fund. The
48 funders provided support in the form of salary for authors [J.D.D; P.P.D; C.V.M], travels,
49 laboratory consumables and analytical costs, but did not have any additional role in the study
50 design, data collection and analysis, decision to publish, or preparation of the manuscript.

51 **Data Availability Statement**

52 The data that support the findings of this study are available at the following links:
53 demultiplexed FastQ files for all five samples can be found under BioProject [PRJNA703741](#) and
54 BioSample accession numbers: [SAMN18024369](#) (BC01), [SAMN18024370](#) (BC02),
55 [SAMN18024371](#) (BC03), [SAMN18024372](#) (BC04), [SAMN18024373](#) (BC05). The intermediate
56 bioinformatics files (medaka.bam; medaka.bam.stats) and final consensus sequences
57 (medaka.fasta) from partial TiLV segment 1 amplicons combined analysis (620 bp and 274 bp)
58 and random 274 bp analysis with subsamples for 1000, 500, 100, and 50 reads, with reference
59 fasta sequences used for both analyses can be found under Zenodo.org dataset DOI
60 [10.5281/zenodo.4556414](#).

61 **Conflict of interest statement**

62 The authors declare no conflict of interest. WorldFish, CIAT and IFPRI have no commercial
63 interest or collaboration with Nanopore and there is no intention of the research to promote any
64 commercial products.

65 **Author contributions**

66 Conceptualization, J.D.D., S.S., H.T.D.; investigation, S.T., J.D.D., P.P.D., H.T.D., S.S.; formal
67 analysis, J.D.D., H.M.G., P.K.; methodology, S.S., H.T.D., S.T., J.D.D., H.M.G.; P.K.;
68 supervision; S.S., H.T.D., J.D.D.; writing - original draft, J.D.D., H.T.D.; review & editing, all.
69 All authors have read and agreed to the current version of the manuscript.

70 **Ethics approval statement**

71 No animal ethic approval was required since all RNA templates used in this study derived from
72 archived samples.

73 **Abstract**

74 Infectious diseases represent one of the major challenges to sustainable aquaculture
75 production. Rapid, accurate diagnosis and genotyping of emerging pathogens during early-
76 suspected disease cases is critical to facilitate timely response to deploy adequate control
77 measures and prevent or reduce spread. Currently, most laboratories use PCR to amplify
78 partial pathogen genomic regions, occasionally combined with sequencing of PCR
79 amplicon(s) using conventional Sanger sequencing services for confirmatory diagnosis. The
80 main limitation of this approach is the lengthy turnaround time. Here, we report an innovative
81 approach using a previously developed specific PCR assay for pathogen diagnosis combined
82 with a new Oxford Nanopore Technologies (ONT)-based amplicon sequencing method for
83 pathogen genotyping. Using fish clinical samples, we applied this approach for the rapid
84 confirmation of PCR amplicon sequences identity and genotyping of tilapia lake virus
85 (TiLV), a disease-causing virus affecting tilapia aquaculture globally. The consensus
86 sequences obtained after polishing exhibit strikingly high identity to references derived by
87 Illumina and Sanger methods (99.83-100%). This study suggests that ONT-based amplicon
88 sequencing is a promising platform to deploy in regional aquatic animal health diagnostic
89 laboratories in low and medium income countries, for fast identification and genotyping of
90 emerging infectious pathogens from field samples within a single day.

91

92 **Keywords:** Nile tilapia (*Oreochromis niloticus*), Red tilapia (*Oreochromis* spp.), Tilapia lake
93 virus, semi-nested RT-PCR, Oxford Nanopore Technologies, genotyping, bioinformatics and
94 phylogenetic analyses.

95

96

97

98

99

100

101

102

103

104

105

106

107

108

109

110

111

112 1 | INTRODUCTION

113 Aquaculture is one of the fastest growing food production sectors and is of increasing
114 importance to global food security. This is particularly true in low income, food deficit
115 countries, where it plays a significant role in livelihood and subsistence. However, the
116 sustainability and expansion of the sector is hampered by disease epidemics. Endemic and
117 emerging infectious diseases (Brummett et al., 2014), pose major animal health issues and
118 economic losses, affecting millions of smallholders (Subasinghe et al., 2019; FAO, 2020).

119 Tilapia are the second most important aquaculture species (in volume) produced globally,
120 with an industry value of \$9.8 billion annually (FAO, 2020). Intensification of tilapia
121 production has driven the emergence of diseases through the translocation of
122 asymptotically infected animals (Rodgers et al., 2011; Jansen et al., 2019; Dong et al.,
123 2017a).

124 Rapid and accurate diagnosis of aquatic pathogens is a central pillar to any successful
125 national aquatic animal health strategy, helping key aquaculture value chain actors to select
126 disease-free fish broodstock, disseminate clean seeds, conduct pathogen surveillance, confirm
127 the aetiological agent of disease outbreaks and prevent their further spread to neighbouring
128 farms, regions and countries. This is especially important for viruses considering the lack of
129 completely effective prophylactic treatments and vaccines for most viral pathogens of fish
130 (Crumlish, 2017; Ninawe et al., 2017).

131 On suspicion of viral disease, the first recommended procedure is to demonstrate clinical
132 pathology via simple observations of abnormal behaviours and external/internal clinical
133 signs. Based on presumptive diagnosis using clinical signs and additional metadata collected
134 from farmer around the disease outbreak, rapid molecular tests (such as PCR, qPCR, LAMP,
135 or strip test kits) targeting priority pathogens can be done. Presence of viable viral particles in
136 clinical samples can be further confirmed by culture in a permissive cell line but this can take
137 days to weeks.

138 For farmed aquatic animals, molecular techniques, e.g., PCR, to confirm the presence of viral
139 nucleic acids (DNA/RNA) are preferred because they yield much faster presumptive
140 diagnosis. Occasionally, amplification products from semi-nested PCRs are Sanger
141 sequenced in order to derive sequence information for genotyping, which may be used for
142 epidemiological tracking and implementation of evidence-based biosecurity actions.
143 Amplicon sequencing is also useful for confirmatory diagnosis to rule out possible false
144 positive results, where less specific methods such as non-nested PCR or LAMP are used.
145 Indeed, OIE recommends amplicon sequencing where non-nested PCR methods are
146 employed, such as those recommended for diagnosis of Koi Herpes Virus (OIE, 2019).

147 Due to scarcity of sequencing facilities, with associated transport and queueing times, this
148 process can take a few days from sample to sequence results. Unfortunately, in many low and
149 middle-income countries (LMICs), clinical samples from disease outbreaks have to be sent
150 overseas due to lacking of locally available sequencing capacity or limited access to specialist
151 laboratories.

152 While Sanger sequencing remains the current preferred sequencing platform to produce
153 accurate short read sequence data, it is time consuming and depends on the availability and
154 accessibility of Sanger's sequencing machine where needed. In addition, its analysis is
155 somewhat laborious and may require manual inspection of the chromatogram. Second and
156 third generation sequencing platforms such as Ion Torrent, Illumina and PacBio are
157 extremely powerful for genomic sequencing of aquatic pathogens, but require substantial

158 capital investment and major laboratory infrastructure. Nevertheless, they have been used to
159 study viruses affecting global fish aquaculture, such as TiLV, piscine reovirus (PRV), piscine
160 myocarditis virus (PMCV), salmonid alphavirus (SAV), infectious salmon anaemia virus
161 (ISAV) (Gallagher et al., 2018; Nkili-Meyong et al., 2016).

162 The MinION/Flongle sequencing platform from Oxford Nanopore Technologies (ONT)
163 offers a simple low-cost portable device for generating real-time sequence data. The low
164 equipment cost, and particularly the lack of requirement for a well-equipped laboratory
165 facility, makes MinION particularly attractive for genomic sequence data-driven management
166 and control of aquatic pathogens in remote locations in LMIC. In this study, we explored the
167 capability and advantage of ONT-based amplicon sequencing coupled with simple
168 bioinformatics analyses for rapid and accurate consensus sequences generation for
169 genotyping of TiLV, the causative agent of syncytial hepatitis of tilapia, a disease affecting
170 tilapia aquaculture in over 16 countries (Taengphu et al., 2020).

171 TiLV is an enveloped, negative-sense, single-stranded RNA virus that contains 10 genomic
172 segments ranging from 465 to 1641 bp, with a total genome size of 10,323 bp (Bacharach et
173 al., 2016), encoding 14 predicted proteins (Acharya et al., 2019). The virus was recently re-
174 classified as a new genus *Tilapinevirus*, the sole genus under the new family *Amnoonviridae*
175 in the order *Articulavirales* (ICTV, 2020).

176 When new viruses (such as TiLV) emerge in aquaculture, non-validated PCR and RT-PCR
177 methods appear very quickly after first detection of the viral diseases. Several TiLV PCR
178 detection assays have been developed, including RT-PCR (Eyngor et al., 2014), nested RT-
179 PCR (Kembou Tsofack et al., 2017), semi-nested RT-PCR (Taengphu et al., 2020; Dong et
180 al., 2017b; Castañeda et al., 2020), RT-qPCR (Tattiyapong et al., 2018; Waiyamitra et al.,
181 2018) and RT-LAMP (Phusantisampan et al., 2019; Yin et al., 2019). However with no
182 validated OIE approved assays for TiLV, sequencing of amplicons can provide robust
183 supporting evidence that the disease has been detected. For this study, we chose a semi-
184 nested RT-PCR method (Taengphu et al., 2020) targeting TiLV segment 1, as its sensitivity is
185 reported to be 100 times higher than a previous TiLV segment 3-based protocol (Dong et al.,
186 2017b), and because TiLV genomic segment 1 amplicons derived from that study (Taengphu
187 et al., 2020) have been used for genotyping of TiLV

188 Here, we report successful use of the semi-nested RT-PCR for diagnosis of TiLV coupled
189 with Nanopore sequencing of amplicons for rapid identification and preliminary genotyping
190 of TiLV. We also discuss the range of possible practical applications and implications of
191 Nanopore sequencing, as a portable platform for robust molecular field diagnostics
192 investigations into the origin and spread of other aquaculture pathogens of economic
193 significance.

194

195

196 **2 | MATERIALS AND METHODS**

197 **2.1 | Workflow**

200 The diagnostic workflow from sample collection from farmed moribund fish, extraction of
201 nucleic acid, semi-nested RT-PCR, library preparation, Nanopore sequencing and data
202 analysis is described in Figure 1.

203

204 **2.2 | RNA samples and reference sequences**

205

206 We used five archived RNA templates extracted from clinical Nile tilapia (*Oreochromis*
207 *niloticus*, Linnaeus) and red tilapia (*Oreochromis* spp.) specimens and from E-11 permissive
208 cell line used for TiLV propagation (Table 1). All five samples were previously confirmed to
209 be TiLV positive. The samples were originally isolated from specimens collected in Thailand
210 (BC01 and BC03), Bangladesh (BC02), and Peru (BC04 and BC05) as described in previous
211 reports (Debnath et al., 2020; Taengphu et al., 2020). Table 1 also includes fourteen full-
212 length TiLV segment 1 reference sequences retrieved from NCBI. The NCBI reference
213 sequences originated from tilapia specimens collected from Thailand, Bangladesh, Peru,
214 Ecuador, Israel and the USA between 2011 and 2018, and were used for sequence alignment
215 and phylogenetic analysis with the amplicon consensus sequences generated in this study.

216

217 **2.3 | Semi-nested RT-PCR**

218

219 Partial regions of the TiLV segment 1 genome were amplified by semi-nested RT-PCR as
220 described previously (Taengphu et al., 2020). Five microliters of the second round PCR
221 products were analyzed by electrophoresis on a 1% agarose gel stained with ethidium
222 bromide solution. The remaining 20 µL reaction volume from the second round PCR was
223 purified for each sample on a NucleoSpin Gel and PCR Clean-up column (Macherey-Nagel)
224 and eluted with 20 µL of the kit elution buffer (5 mM Tris-HCl, pH 8.5). The purified
225 products were quantified using Qubit dsDNA Broad Range kit (Qiagen) with a Qubit 3.0
226 fluorometer prior to Nanopore multiplex library preparation.

227

228 **2.4 | Library preparation of TiLV PCR products for Nanopore sequencing**

229

230 To prepare the TiLV library, the ligation sequencing kit (SQK-LSK109) and the native
231 barcoding expansion 1-12 kit (EXP-NBD104) were used according to the Oxford Nanopore
232 Technologies (ONT) standard protocols adapted for the Flongle flow cell. We used 250 ng
233 PCR products for each sample (BC01-BC05), one unique native barcode (BC) per sample
234 and washed the library of pooled barcoded samples with the Short Fragment Buffer (SFB)
235 just before the elution step at the end of the protocol. DNA concentrations were determined
236 between each step using the Qubit assay. The prepared TiLV library was loaded as per the
237 standard protocol onto a Flongle flow cell (FLO-FLG106)— with 29 active pores— fitted to
238 a Flongle adapter (FLGIntSP) for MinION.

239

240 **2.5 | Data acquisition and basecalling**

241

242 Control of the MinION and high accuracy base-calling data acquisition were performed
243 offline in real-time using the stand-alone MinIT (MNT-001): a pre-configured compute
244 module with MINKNOW software version (19.05.02). The raw Fast5 files were subsequently

245 re-basecalled and demultiplexed using the latest Guppy version (v.4.4.1) in high accuracy
246 mode to further improve base-calling accuracy.
247

248 **2.6 | Bioinformatics analyses for TiLV amplicons consensus sequences generation**

249

250 The base-called and demultiplexed FastQ files were individually assessed using NanoStat
251 (De Coster et al., 2018). Raw reads were aligned to a primer-trimmed TiLV Segment 1 gene
252 region (Accession Number: [MN687685.1](#)) using Minimap2 v2.17 (-ax map-ont –
253 secondary=no). High quality reads (qscore of 10 and above) with read length of more than
254 500 bp were selected for consensus generation, since they were assumed to have been
255 generated from the sequencing of the 620 bp amplicons (first round PCR products). Briefly,
256 the filtered reads were re-aligned to the reference sequence using Minimap2 v2.17 followed
257 by one round of polishing with RACON v1.4.20 (-m 8 -x -6 -g -8 -w 250) and then
258 Medaka_consensus v1.1.3 (-m r941_min_high_g360). To examine the effect of sequencing
259 coverage (or read depth) on consensus accuracy, high-quality reads (qscore of 10 and above)
260 ranging from 270 to 320 bp that aligned to the 274 bp amplicons (semi-nested PCR products)
261 were randomly subsampled for 1000, 500, 100, and 50 reads and used for consensus
262 generation as described above. Subsampling of the reads was done with seqtk v1.2 using the
263 same initial seed number as reservoir sampling for each number of reads to be subsampled,
264 where all reads randomly selected with equal probability.
265

266 Pair-wise nucleotide similarity of the consensus sequences against their respective reference
267 sequences were calculated using NCBI BlastN. To obtain the number of reads sequenced
268 over time, ‘Sequencing start time’ was extracted from every sequence identifier using grep
269 and cut commands. The extracted data were used to generate histograms representing the
270 number of reads generated every 5 min.
271

272 **2.7 | Alignment of TiLV segment 1 amplicon consensus sequences to public references 273 for phylogenetic analyses**

274

275 A total of 24 TiLV segment 1 sequences were used for phylogenetic analyses, including five
276 consensus sequences derived from this study first round PCR products (620 bp), five from
277 this study semi-nested PCR products (274 bp) and 14 full-length (1560 bp) TiLV segment 1
278 reference sequences retrieved from GenBank database ([Table 1](#)). The latter were trimmed to
279 620 bp and 274 bp. Alignments were made in Jalview (Waterhouse et al., 2009) using the
280 web service Muscle v3.8.31 (web service) defaults parameters (Edgar, 2004). The non-
281 aligned regions and the 5' and 3' primer binding sites were trimmed resulting in 577 bp and
282 231 bp sequences from the 620 bp and 274 bp sequences of interest, respectively.
283 Phylogenetic trees were built in IQ-TREE (v.1.6.12) using the Maximum Likelihood
284 approach. The first tree using the five 577 bp consensus sequences and 14 reference
285 sequences trimmed to 577 bp. The second tree using the five 577 bp consensus sequences
286 trimmed to 231 bp, five original 231 bp consensus sequences and 14 reference sequences
287 trimmed to 231 bp. Given the lack of a closely related outgroup for TILV, we opted to root
288 the trees using the mid-point rooting method (Wohl et al., 2016) to avoid outgroup long-
289 branches in the trees.
290

291

292

293

294

295

296 3 | RESULTS

297

298 3.1 | TiLV positive clinical samples confirmed by PCR

299

300 The segment 1 semi-nested PCR assay confirmed that the five samples used in this study
301 (Table 1) were TiLV positive (Figure S1). Bands at 620 bp are the product of the first round
302 RT-PCR, and bottom bands at 274 bp are the product of the second round semi-nested PCR.
303 Samples BC01, BC02, BC03, and BC05 that produced both the 620 and 274 bp products
304 were considered as “heavy infection” and sample BC04 that only generated a 274 bp band
305 was considered as “light infection”. Two heavy infected samples (BC01 and BC03) yielded
306 an additional band at around 1-1.1 kb which was derived from cross-hybridized amplified
307 products (Figure S1) as indicated previously (Taengphu et al, 2020).

308

309 3.2 | Sequencing output and rapid bioinformatics analyses

310

311 The sequencing run on the Flongle flow cell generated 174.69K reads with 114.99 Mb of
312 estimated bases and 93.53 Mb base called. Depending on the sample, 517 to 964 reads were
313 generated in the first 5 min of the run (Figure S2). Those numbers gradually decreased with
314 reduction of available active sequencing pores to drop on average below 116 reads per
315 sample after 4 h, 15 reads per sample after 5h and no more reads produced past 6 h of the
316 sequencing run (Figure S2). The number of reads sequenced over time will vary depending
317 on flow cell type (Minion vs Flongle), flow cell pore count, library preparation quality, and
318 amplicon size. Histograms of the read length distribution—for all five samples—indicate two
319 main peaks at 620 bp and 274 bp (Figure S3). BC01 and BC02 had a higher peak at 620 bp
320 and BC03, BC04 and BC05 at 274 bp. Our PCR results and sequence data both confirmed the
321 semi-quantitative nature of this (ONT)-based amplicon sequencing approach that can
322 differentiate between heavy, medium and light TiLV infected samples (Figure S1 and S3).

323

324 Given that this is an amplicon sequencing, there is no *de novo* assembly procedure, which is
325 typically one of the more memory-consuming step in bioinformatics. The alignment of raw
326 Nanopore reads to the TiLV reference sequence using Minimap2 took less than 10 seconds to
327 complete while the polishing steps consisting of RACON and MEDAKA took about 5-10
328 minutes per sample depending on their read depth with lower read depth leading to faster
329 consensus generation. In this study, the entire pipeline starting from basecalled FastQ files to
330 consensus generation, sequences alignment and phylogenetic analyses was performed on a
331 typical office laptop (ASUS VivoBook, AMD Ryzen 5, 8 GB RAM).

332

333 3.3 | Accurate consensus generation for TiLV identification

334

335 The average percentage identity of the adapter-trimmed and quality-filtered (qscore of 10 and
336 above) Nanopore reads against their respective Sanger TiLV segment 1 references ranged
337 between 92.5 and 93.2% (Table S1 and Table S2). Out of the five samples, only the Thai
338 BC03 and Peruvian BC04 had their full length TiLV segment 1 region (1560 bp) previously
339 Sanger sequenced: TH-2018-N and PE-2018-F3-4, respectively (Table 1 and Table 2). We
340 confirmed 100% nucleotide identity of the 577 bp amplicon of the Thai BC03 and Peruvian
341 BC04 consensus to their original references (Table 2A). The Thai BC01 (viral isolate from
342 Nile tilapia infected tissue sample propagated in E-11 cell line) was also 100% identical to
343 BC03 (isolated from red tilapia) but BC01 came from a different farm seven months later,

344 suggesting that this variant is capable of infecting multiple species in different farming areas
345 of Thailand.

346

347 The 577 bp BC02 Bangladeshi consensus sequence was 99.83% identical to BD-2017-181
348 (Table 2A). The single SNP (A instead of G) in position 334 (Figure 2A) was further
349 assessed in Integrative Genomics Viewer (IGV) using BC02.medaka.bam file (read depth)
350 with final BC02.medaka.fasta sequence. The SNP was confirmed to be amplicon-specific,
351 partitioned between 274 and 620 amplicons (Figure 2C). Full summary of sequencing
352 statistics for mixed amplicons (274 and 620 bp) derived from NanoStat can be found in Table
353 S1.

354 A BlastN analysis of the Peruvian 577 bp BC05 consensus sequence returned 99.83% identity
355 to PE-2018-F3-4 (Table 2A), with alignment of BC05 and PE-2018-F3-4 showing only one
356 SNP (A instead of a G) in position 347 (Figure 2B). This SNP was confirmed in IGV, which
357 revealed consistent base call of an Adenine (A) in the majority of the reads
358 (BC05.consensus.bam file) with only one Guanine (G) corresponding to a homopolymer base
359 calling error (Figure 2D). While both BC04 and BC05 were collected in 2018, they came
360 from different farms. This indicates the presence in Peru of at least two TiLV variants at the
361 time of sampling.

362 **3.4 | Sequencing coverage for reliable genotyping**

363 Consensus sequences (231 bp) generated from the random subsampling of 1000, 500, 100
364 and 50 reads from the same sample are 100% similar in all cases (Table 2B). NanoStat
365 summary statistics of sequencing output for 274 bp and sub-sampling analysis are presented
366 in Table S2.

367 **3.5 | Phylogenetic analysis of TiLV segment 1 amplicon consensus**

368 Two phylogenetic trees were generated. The first tree comparing the five 577 bp consensus
369 sequences (this study) with NCBI reference sequences (Table 1) trimmed to 577 bp (Figure
370 3A). The second tree includes the same five 577 bp consensus sequences trimmed to 231 bp,
371 with the five original 231 bp consensus sequences (this study) compared with NCBI
372 reference sequences trimmed to 231 bp (Figure 3B).

373

374 The five 577 bp consensus sequences generated in this study clustered those TiLV isolates
375 into two separate clades, namely Thai (C1) and Israel 2012 (Figure 3A). The Thai C1 clade
376 was divided into two sub-clades: C1a and C1b. Clade C1a contains BC01 and BC03 Thai
377 isolates both clustering closely with TH-2018-N. Clade C1b includes BC02 that is most
378 similar to BD-2017-181. The Israeli 2012 clade comprises BC04 and BC05 Peruvian isolates
379 clustering with PE-2018-F3-4. IL-2011-Til-4-2011 forms a monophyletic clade outside of
380 “Israel 2012” clade (Figure 3A). Reference sequence for TH-2018-K—when trimmed from
381 1560 bp to 577 bp—positions TH-2018-K outside the Thai (C1) clade (Figure 3A).

382

383 In the tree derived from alignment of 231 bp sequence data (Figure 3B), the BC01 and BC03
384 Thai isolates still cluster in the Thai C1a clade. The 231 bp consensus sequence of the BC02
385 Bangladeshi isolate still places it in the C1b Thai sub-clade but the shorter consensus
386 sequences (231 bp) of the BC04 and BC05 Peruvian isolates, now make those two isolates
387 more closely related to the Israeli 2011 clade (IL-2011-Til-4-2011) (Figure 3B). Trimmed
388 reference sequences (1560 bp to 231 bp) for TH-2018-K and TH-2016-TV7 isolates now
389 position them outside the Thai (C1) clade (Figure 3B).

390

391

392

393

394

395

396 4 | DISCUSSION

397

398 The read accuracy of MinION data has been a disadvantage of the platform when compared
399 with Sanger or Illumina sequencing. However, it has greatly improved with advances in flow
400 cell chemistry, base-calling software and consensus accuracy. With sufficient read depth, a
401 consensus sequence with adequate accuracy for genotyping can now be generated quickly
402 with the right bioinformatics tools without requiring high computing capacity. With the right
403 capacity building and training of molecular diagnosticians and aquaculture technicians, our
404 proposed workflow and bioinformatics analytical pipeline can be adopted in targeted
405 countries to generate similar results.

406

407 While we cannot ascertain if the SNP identified in the Bangladeshi BC02 isolate is real due to
408 the lack of Sanger sequencing data for the same PCR product, it may be a genuine SNP
409 variation from the viral population sequenced. BC02 was collected on the same farm and at
410 the same time but not from the same diseased fish that was used to derive the whole genome
411 of BD-2017-181: one of the only four publicly available TiLV segment 1-reference
412 sequences from Tilapia in Bangladesh (Debnath et al., 2020). We know that viral RNA-
413 dependent RNA polymerases are error-prone, with misincorporation of a wrong nucleotide
414 estimated every 10,000-1,000,000 nucleotides polymerized depending of viral species
415 (Sanjuán et al., 2010). This high rate of mutation comes from the lack of proofreading ability
416 in RNA polymerases (Steinhauer et al., 1992). Given the size of the TiLV RNA genome of
417 10,323 bases, a mutation rate of 1 in 10,000 would mean an average of 1 mutation in every
418 replicated genome. If a single tilapia cell is infected with TiLV and produces 10,000 new
419 viral particles, this mutation frequency means in theory that about 10,000 new TiLV variants
420 have been produced. This incredible high mutation rate explains why RNA viruses evolve so
421 quickly. Viral populations even in a single infection are not homogeneous and will be mixed
422 at any point in time during the infection. What is sequenced from the PCR is usually an
423 amplification of the most populous variant at the time sampled with the additional stochastic
424 effect of which templates amplify in the first few rounds of the PCR, plus the possible (but
425 rare) misincorporation of a dNTP by the PCR polymerase early in the amplification.

426 Given the relatively high sequence identity (> 92.5%) at the single Nanopore read level
427 observed for the TiLV amplicons used in this study, real-time analysis of base-called and
428 demultiplexed Nanopore barcoded reads will allow estimation of the minimum sequencing
429 time (or number of reads) required to achieve a positive identification, which should be
430 occurring in just a few seconds depending on the number of samples being sequenced, flow
431 cell pore occupancy, library preparation quality and computing capability. In this study, an
432 amplicon read depth of 50 X is sufficient to generate a TiLV amplicon consensus sequence
433 with high accuracy suitable for preliminary genotyping. The read depth requirement may
434 vary depending on the sequence composition, e.g., homopolymer content that are more prone
435 to Nanopore sequencing error. A study using Nanopore to sequence the complete genome of
436 salmonid alphavirus (SAV1) reported similarly low sequence coverage to generate highly
437 accurate consensus (Gallagher et al., 2018), where authors needed as little as 20 X coverage
438 to get a consensus 99% similar to Sanger reference, while 1,000 X coverage led to 99.97%
439 similarity.

440 The phylogenetic tree topology using consensus sequences of 577 bp is mostly in agreement
441 with the literature, since it classifies the Thai and Bangladeshi consensus (BC01, BC02 and
442 BC03) into the correct “Thai” clade. On the contrary, the Peruvian isolates (BC04 and BC05)
443 are now more closely related to IL-2012-AD-2016 (Israeli 2012 clade)—where in other
444 studies that used the full-length sequences (1560 bp) of TiLV segment 1—those normally
445 cluster them into the “Israeli 2011” clade (Debnath et al., 2020; Taengphu et al., 2020). The
446 differences observed can be explained by the different sequence lengths used between
447 studies. Here we used shorter amplicons (231 and 577 bp) as opposed to the full-length TiLV
448 segment 1 sequences (1560 bp) used in the two aforementioned studies, where longer
449 sequences provide more accurate resolution.

450
451 While short amplicons seem suitable for preliminary TiLV genotyping, a recent study
452 analyzed each individual TiLV genome segment separately, resulting in different
453 phylogenetic trees with high estimation uncertainties (Chaput et al., 2020). The authors’
454 suggested exercising caution when using phylogenetic analysis to infer geographic origin and
455 track the movement of TiLV, and recommend using whole genomes for phylogeny wherever
456 possible. To avoid having to sequence complete viral genomes, further sequencing data may
457 be enough to identify regions of the genome that are descriptive—similar to multi-locus
458 sequence typing scheme used to identify prokaryote lineages. Another good example on the
459 need for complete genomic sequences has recently been described in a study conducted by
460 (Thawornwattana et al., 2021), which looked at eight TiLV complete genomes from Thailand
461 collected between 2014 and 2019. Those genomes were analyzed by Bayesian inference
462 allowing for estimation of virus evolutionary timescales, rates and global population
463 dynamics since the early origin of TiLV. This was only possible using complete genomic
464 sequences.

465
466 The inherent nature of segmented virus such as TiLV limits one of the main benefits of
467 Nanopore sequencing, which is to generate a complete viral genome with a few small
468 overlapping PCR amplified regions. Salmonid alphavirus (SAV), a ~12 kb non-segmented,
469 single-stranded, positive-sense RNA virus is the only fish virus genome successfully
470 sequenced by Nanopore and was confirmed for assembly accuracy against Sanger verified
471 reference sequence (Gallagher et al., 2018). To date, the 19 complete genomes of TiLV have
472 been sequenced by Sanger (Debnath et al., 2020; Thawornwattana et al., 2021) and, Illumina
473 (Chaput et al., 2020; Subramaniam et al., 2019; Al-Hussinee et al., 2018), but none have been
474 sequenced by Nanopore. To achieve this will require amplifying all 10 segments individually
475 by RT-PCR using different primer pairs and cycling conditions and we accept that this
476 process may be time-consuming and possibly challenging given the relatively high nucleotide
477 divergence among TiLV strain from different lineages.

478
479 This study serves as a “proof of concept” using primers previously used to detect TiLV to
480 reliably amplify the TiLV segment 1 gene fragment for Nanopore sequencing. That said,
481 design of new set of universal primers to recover longer regions if not, the entire TiLV
482 segment 1 region or more ambitiously multiple complete TiLV genome segments for
483 Nanopore sequencing will be considered. The accuracy of Nanopore (MINION/Flongle)
484 depends largely on the sequence composition rather than the sequence length. Generally,
485 amplicons generated from genomic regions with longer homopolymer length will be
486 sequenced less accurately at the single-read level. However, with sufficient read depth, a
487 consensus with high accuracy can be generated with proper polishing step as shown in this
488 study.

489 The choice of whether to sequence short amplicons, entire segment(s) or the whole genome
490 of TiLV will depend on the specific need. For simple and rapid confirmatory PCR diagnosis
491 results with some phylogeny inferences for preliminary genotyping, we have shown that
492 using 274 and 620 bp amplicons from TiLV segment 1 works very well but for high-
493 resolution epidemiological and evolutionary analyses a whole genome approach would be
494 required.

495 PCR-MinION is a rapid method to generate accurate consensus sequences for TiLV
496 identification and genotyping. This method currently takes less than 12 h from clinical
497 sample collection to sequence results. We show that low read depth (or coverage) does not
498 affect the accuracy of 274 bp consensus generation, hence the possibility to further reduce
499 sequencing time. In the hands of trained and skilled end-users, this device with the specific
500 sample preparation protocols and our analytical workflow will enable point-of-care testing
501 and sequencing in remote locations, helping teams of governmental and supra-national
502 institutions during disease outbreak investigations. Such application of Nanopore has been
503 successfully applied to study human epidemics such as Ebola virus in remote areas of West
504 Africa (Hoenen et al., 2016), the Zika virus in hard to reach regions of Brazil (Faria et al.,
505 2016). More recently, the technology was used to sequence and identify SARS-CoV-2, the
506 virus causing the COVID-19 pandemic (Wang et al., 2020).

507
508 In conclusion, applied to aquatic animal production systems, our approach coupled to routine
509 diagnostic PCR, can offer a rapid and deployable mobile solution for early genotyping of
510 TiLV and other newly emerging infectious diseases of economics importance. Genotyping
511 provides crucial insights into the genetics of disease outbreaks and their possible origin(s).
512 Having demonstrated that this workflow can provide genotyping information for TiLV short
513 fragments, future work will aim at larger amplicons (> 1 kb) for finer epidemiological
514 tracking of pathogen populations. In addition, sequencing of multiple amplicons from
515 different samples in a single run offers scalability and the opportunity to reduce per-sample
516 costs even further. With the deployment of portable real-time DNA sequencing platform
517 across national reference and regional laboratories in LMIC, trained laboratory technicians
518 will be able to genetically screen clinical samples from routine surveillance programs and
519 disease outbreak investigations. Through genomic sequence data-driven management,
520 competent authorities can precisely define movement controls of aquatic animals, and
521 provide recommendations to farmers to take appropriate actions. This will minimize the
522 introduction, and spread of TiLV and other infectious diseases of farmed aquatic animals,
523 contributing to both economic and food security.

524

525

526

527

528

529

530

531

532

533

534

535

536

537

538

539

540

541

542

543 **REFERENCES**

544

545 Acharya, V., Chakraborty, H. J., Rout, A. K., Balabantaray, S., Behera, B. K., & Das, B. K.
546 (2019). Structural characterization of open reading frame-encoded functional genes
547 from tilapia lake virus (TiLV). *Molecular Biotechnology*, *61*, 945–957.
<https://doi.org/10.1007/s12033-019-00217-y>

548 Al-Hussinee, L., Subramaniam, K., Ahsan, M. S., Keleher, B., & Waltzek, T. B. (2018).
549 Complete genome sequence of a tilapia lake virus isolate obtained from Nile tilapia
550 (*Oreochromis niloticus*). *Genome Announcements*, *6*, e00580-18.
<https://doi.org/10.1128/genomeA.00580-18>

551 Bacharach, E., Mishra, N., Briese, T., Zody, M. C., Kembou Tsafack, J. E., Zamostiano, R.,
552 Berkowitz, A., Ng, J., Nitido, A., Corvelo, A., Toussaint, N. C., Abel Nielsen, S. C.,
553 Hornig, M., Del Pozo, J., Bloom, T., Ferguson, H., Eldar, A., & Lipkin, W. I. (2016).
554 Characterization of a novel orthomyxo-like virus causing mass die-offs of tilapia.
555 *MBio*, *7*, e00431-16. <https://doi.org/10.1128/mBio.00431-16>

556 Brummett, R. E., Alvial, A., Kibenge, F., Forster, J., Burgos, J. M., Ibarra, R., St-Hilaire, S.,
557 Chamberlain, G. C., Lightner, D. V., Khoa, L. V., Hao, N. V., Tung, H., Loc, T. H.,
558 Reantaso, M., Wyk, P. M. V., Chamberlain, G. W., Towner, R., Villarreal, M.,
559 Akazawa, N., ... Nikuli, H. L. (2014). Reducing disease risk in aquaculture.
560 Agriculture and environmental services discussion paper; no. 9. *Washington, D.C.: World Bank Group*. (119 pp). Retrieved from
<http://documents.worldbank.org/curated/en/110681468054563438/Reducing-disease-risk-in-aquaculture>

561 Castañeda, A. E., Feria, M. A., Toledo, O. E., Castillo, D., Cueva, M. D., & Motte, E. (2020).
562 Detection of tilapia lake virus (TiLV) by seminested RT-PCR in farmed tilapias from
563 two regions of Peru. *Revista de Investigaciones Veterinarias del Perú (RIVEP)*, *31*,
564 e16158. <https://doi.org/10.15381/rivep.v31i2.16158>

565 Chaput, D. L., Bass, D., Alam, Md. M., Al Hasan, N., Stentiford, G. D., Van Aerle, R.,
566 Moore, K., Bignell, J. P., Haque, M. M., & Tyler, C. R. (2020). The segment matters:
567 probable reassortment of tilapia lake virus (TiLV) complicates phylogenetic analysis
568 and inference of geographical origin of new isolate from Bangladesh. *Viruses*, *12*,
569 258. <https://doi.org/10.3390/v12030258>

570 Crumlish, M. (2017). Bacterial diagnosis and control in fish and shellfish. In B. Austin & A.
571 Newaj-Fyzul (Eds.), *Diagnosis and control of diseases of fish and shellfish* (pp. 5–18).
572 John Wiley & Sons, Ltd. <https://doi.org/10.1002/9781119152125.ch2>

573 De Coster, W., D'Hert, S., Schultz, D. T., Cruts, M., & Van Broeckhoven, C. (2018).
574 NanoPack: visualizing and processing long-read sequencing data. *Bioinformatics*, *34*,
575 2666–2669. <https://doi.org/10.1093/bioinformatics/bty149>

576 Debnath, P. P., Delamare Deboutteville, J., Jansen, M. D., Phiwsaiya, K., Dalia, A., Hasan,
577 M. A., Senapin, S., Mohan, C. V., Dong, H. T., & Rodkhum, C. (2020). Two-year

583 surveillance of tilapia lake virus (TiLV) reveals its wide circulation in tilapia farms
584 and hatcheries from multiple districts of Bangladesh. *Journal of Fish Diseases*, 43,
585 1381–1389. <https://doi.org/10.1111/jfd.13235>

586 Dong, H. T., Ataguba, G. A., Khunrae, P., Rattanarojpong, T., & Senapin, S. (2017a).
587 Evidence of TiLV infection in tilapia hatcheries from 2012 to 2017 reveals probable
588 global spread of the disease. *Aquaculture*, 479, 579–583.
589 <https://doi.org/10.1016/j.aquaculture.2017.06.035>

590 Dong, H. T., Siriroob, S., Meemetta, W., Santimanawong, W., Gangnonngiw, W., Pirarat, N.,
591 Khunrae, P., Rattanarojpong, T., Vanichviriyakit, R., & Senapin, S. (2017b).
592 Emergence of tilapia lake virus in Thailand and an alternative semi-nested RT-PCR
593 for detection. *Aquaculture*, 476, 111–118.
594 <https://doi.org/10.1016/j.aquaculture.2017.04.019>

595 Edgar, R. C. (2004). MUSCLE: multiple sequence alignment with high accuracy and high
596 throughput. *Nucleic Acids Research*, 32, 1792–1797.
597 <https://doi.org/10.1093/nar/gkh340>

598 Eyangor, M., Zamostiano, R., Kembou Tsofack, J. E., Berkowitz, A., Bercovier, H., Tinman,
599 S., Lev, M., Hurvitz, A., Galeotti, M., Bacharach, E., & Eldar, A. (2014).
600 Identification of a novel RNA virus lethal to tilapia. *Journal of Clinical Microbiology*,
601 52, 4137–4146. <https://doi.org/10.1128/JCM.00827-14>

602 FAO. (2020). The State of World Fisheries and Aquaculture 2020: Sustainability in action.
603 *FAO*, Rome. <https://doi.org/10.4060/ca9229en>

604 Faria, N. R., Sabino, E. C., Nunes, M. R. T., Alcantara, L. C. J., Loman, N. J., & Pybus, O.
605 G. (2016). Mobile real-time surveillance of Zika virus in Brazil. *Genome Medicine*, 8,
606 97. <https://doi.org/10.1186/s13073-016-0356-2>

607 Gallagher, M. D., Matejusova, I., Nguyen, L., Ruane, N. M., Falk, K., & Macqueen, D. J.
608 (2018). Nanopore sequencing for rapid diagnostics of salmonid RNA viruses.
609 *Scientific Reports*, 8, 16307. <https://doi.org/10.1038/s41598-018-34464-x>

610 Hoenen, T., Groseth, A., Rosenke, K., Fischer, R. J., Hoenen, A., Judson, S. D., Martellaro,
611 C., Falzarano, D., Marzi, A., Squires, R. B., Wollenberg, K. R., de Wit, E., Prescott,
612 J., Safronetz, D., van Doremalen, N., Bushmaker, T., Feldmann, F., McNally, K.,
613 Bolay, F. K., ... Feldmann, H. (2016). Nanopore sequencing as a rapidly deployable
614 Ebola outbreak tool. *Emerging Infectious Diseases*, 22, 331–334.
615 <https://doi.org/10.3201/eid2202.151796>

616 ICTV. (2020). International Committee on Taxonomy of Viruses – Virus Taxonomy: 2020
617 release. (2021, May 17). Retrieved from <https://talk.ictvonline.org/taxonomy/>

618 Jansen, M. D., Dong, H. T., & Mohan, C. V. (2019). Tilapia lake virus: a threat to the global
619 tilapia industry? *Reviews in Aquaculture*, 11, 725–739.
620 <https://doi.org/10.1111/raq.12254>

621 Kembou Tsofack, J. E., Zamostiano, R., Watted, S., Berkowitz, A., Rosenbluth, E., Mishra,
622 N., Briesse, T., Lipkin, W. I., Kabuusu, R. M., Ferguson, H., del Pozo, J., Eldar, A., &
623 Bacharach, E. (2017). Detection of tilapia lake virus in clinical samples by culturing
624 and nested reverse transcription-PCR. *Journal of Clinical Microbiology*, 55, 759–767.
625 <https://doi.org/10.1128/JCM.01808-16>

626 Ninawe, A. S., Hameed, A. S. S., & Selvin, J. (2017). Advancements in diagnosis and control
627 measures of viral pathogens in aquaculture: an Indian perspective. *Aquaculture
628 International*, 25, 251–264. <https://doi.org/10.1007/s10499-016-0026-9>

629 Nkili-Meyong, A. A., Bigarré, L., Labouba, I., Vallaeys, T., Avarre, J.-C., & Berthet, N.
630 (2016). Contribution of next-generation sequencing to aquatic and fish virology.
631 *Intervirology*, 59, 285–300. <https://doi.org/10.1159/000477808>

632 OIE. (2019). Chapter 2.3.7 Infection with koi herpesvirus. In *Manual of diagnostic tests for*

633 aquatic animals. *OIE - World Organisation for Animal Health*. Retrieved May 18,
634 2021, from [https://www.oie.int/en/what-we-do/standards/codes-and-manuals/aquatic-
635 manual-online-access/](https://www.oie.int/en/what-we-do/standards/codes-and-manuals/aquatic-manual-online-access/)

636 Phusantisampan, T., Tattiayapong, P., Mutrakulcharoen, P., Sriariyanun, M., & Surachetpong,
637 W. (2019). Rapid detection of tilapia lake virus using a one-step reverse transcription
638 loop-mediated isothermal amplification assay. *Aquaculture*, 507, 35–39.
639 <https://doi.org/10.1016/j.aquaculture.2019.04.015>

640 Pulido, L. L. H., Mora, C. M., Hung, A. L., Dong, H. T., & Senapin, S. (2019). Tilapia lake
641 virus (TiLV) from Peru is genetically close to the Israeli isolates. *Aquaculture*, 510,
642 61–65. <https://doi.org/10.1016/j.aquaculture.2019.04.058>

643 Rodgers, C. J., Mohan, C. V., & Peeler, E. J. (2011). The spread of pathogens through trade
644 in aquatic animals and their products. *Revue Scientifique et Technique (International
645 Office of Epizootics)*, 30, 241–256. <https://doi.org/10.20506/rst.30.1.2034>

646 Sanjuán, R., Nebot, M. R., Chirico, N., Mansky, L. M., & Belshaw, R. (2010). Viral mutation
647 rates. *Journal of Virology*, 84, 9733–9748. <https://doi.org/10.1128/JVI.00694-10>

648 Steinhauer, D. A., Domingo, E., & Holland, J. J. (1992). Lack of evidence for proofreading
649 mechanisms associated with an RNA virus polymerase. *Gene*, 122, 281–288.
650 [https://doi.org/10.1016/0378-1119\(92\)90216-C](https://doi.org/10.1016/0378-1119(92)90216-C)

651 Subasinghe, R. P., Delamare-Deboutteville, J., Mohan, C. V., & Phillips, M. J. (2019).
652 Vulnerabilities in aquatic animal production. *Revue Scientifique et Technique
653 (International Office of Epizootics)*, 38, 423–436.
654 <https://doi.org/10.20506/rst.38.2.2996>

655 Subramaniam, K., Ferguson, H. W., Kabuusu, R., & Waltzek, T. B. (2019). Genome
656 sequence of tilapia lake virus associated with syncytial hepatitis of tilapia in an
657 Ecuadorian aquaculture facility. *Microbiology Resource Announcements*, 8, e00084-
658 19. <https://doi.org/10.1128/MRA.00084-19>

659 Surachetpong, W., Janetanakit, T., Nonthabenjawan, N., Tattiayapong, P., Sirikanchana, K., &
660 Amonsin, A. (2017). Outbreaks of tilapia lake virus infection, Thailand, 2015–2016.
661 *Emerging Infectious Diseases*, 23, 1031–1033.
662 <https://doi.org/10.3201/eid2306.161278>

663 Taengphu, S., Sangsuriya, P., Phiwsaiya, K., Debnath, P. P., Delamare-Deboutteville, J.,
664 Mohan, C. V., Dong, H. T., & Senapin, S. (2020). Genetic diversity of tilapia lake
665 virus genome segment 1 from 2011 to 2019 and a newly validated semi-nested RT-
666 PCR method. *Aquaculture*, 526, 735423.
667 <https://doi.org/10.1016/j.aquaculture.2020.735423>

668 Tattiayapong, P., Sirikanchana, K., & Surachetpong, W. (2018). Development and validation
669 of a reverse transcription quantitative polymerase chain reaction for tilapia lake virus
670 detection in clinical samples and experimentally challenged fish. *Journal of Fish
671 Diseases*, 41, 255–261. <https://doi.org/10.1111/jfd.12708>

672 Thawornwattana, Y., Dong, H. T., Phiwsaiya, K., Sangsuriya, P., Senapin, S., & Aiewsakun,
673 P. (2021). Tilapia lake virus (TiLV): genomic epidemiology and its early origin.
674 *Transboundary and Emerging Diseases*, 68, 435–444.
675 <https://doi.org/10.1111/tbed.13693>

676 Waiyamitra, P., Tattiayapong, P., Sirikanchana, K., Mongkolsuk, S., Nicholson, P., &
677 Surachetpong, W. (2018). A TaqMan RT-qPCR assay for tilapia lake virus (TiLV)
678 detection in tilapia. *Aquaculture*, 497, 184–188.
679 <https://doi.org/10.1016/j.aquaculture.2018.07.060>

680 Wang, M., Fu, A., Hu, B., Tong, Y., Liu, R., Liu, Z., Gu, J., Xiang, B., Liu, J., Jiang, W.,
681 Shen, G., Zhao, W., Men, D., Deng, Z., Yu, L., Wei, W., Li, Y., & Liu, T. (2020).
682 Nanopore targeted sequencing for the accurate and comprehensive detection of

683 SARS-CoV-2 and other respiratory viruses. *Small*, 16, 2002169.
684 <https://doi.org/10.1002/smll.202002169>

685 Waterhouse, A. M., Procter, J. B., Martin, D. M. A., Clamp, M., & Barton, G. J. (2009).
686 Jalview Version 2—a multiple sequence alignment editor and analysis workbench.
687 *Bioinformatics*, 25, 1189–1191. <https://doi.org/10.1093/bioinformatics/btp033>

688 Wohl, S., Schaffner, S. F., & Sabeti, P. C. (2016). Genomic analysis of viral outbreaks.
689 *Annual Review of Virology*, 3, 173–195. <https://doi.org/10.1146/annurev-virology-110615-035747>

690 Yin, J., Wang, Q., Wang, Y., Li, Y., Zeng, W., Wu, J., Ren, Y., Tang, Y., Gao, C., Hu, H., &
691 Bergmann, S. M. (2019). Development of a simple and rapid reverse transcription–
692 loopmediated isothermal amplification (RT-LAMP) assay for sensitive detection of
693 tilapia lake virus. *Journal of Fish Diseases*, 42, 817–824.
694 <https://doi.org/10.1111/jfd.12983>

695

696

697

698

699

700

701

702

703

704

705

706

707

708

709

710

711

712

713

714

715

716

717

718

719

720

721

722

723

724 **TABLE 1** Details of TiLV samples used in this study (No. 1-5) whose genomic partial
725 segment 1 sequences were compared with NCBI references (no. 6-19) for phylogenetic
726 analysis

No.	Sample code	Date	Origin	Fish host	NCBI Accession no.	References
1	BC01 E-11 cell line day 4	2019	Thailand	Nile tilapia	Not done	This study
2	BC02 Ti Bang 176-1	2017	Bangladesh	Nile tilapia	Not done	This study
3	BC03 S1-18	2018	Thailand	RT fingerling	TH-2018-N (MN687745.1)	This study
4	BC04 m Peru 2018 F3-4	Feb 2018	Peru	Nile tilapia	PE-2018_F3-4 (MK425010.1)	This study
5	BC05 O Peru 2018 F4-5	Feb 2018	Peru	Nile tilapia	Not done	This study
6	IL-2011-Til-4- 2011	May 2011	Israel	Tilapia	KU751814.1	(Eyngor et al., 2014) (Bacharach et al., 2016)
7	IL-2012-AD- 2016	Aug 2012	Israel	HT	KU552131.1	NCBI
8	TH-2016-TV7	May 2016	Thailand	Nile tilapia	KX631936.1	(Surachetpong et al., 2017)
9	EC-2012	Jul 2012	Ecuador	Nile tilapia	MK392372.1	(Subramaniam et al., 2019)
10	TH-2018-K	Aug 2018	Thailand	NT juvenile	MN687755.1	(Thawornwattana et al., 2021)
11	TH-2018-N	Jul 2018	Thailand	RT fingerling	MN687745.1	(Thawornwattana et al., 2021)
12	TH-2019	Feb 2019	Thailand	NT fingerlings	MN687765.1	(Thawornwattana et al., 2021)
13	PE-2018-F3-4	Feb 2018	Peru	Nile tilapia	MK425010.1	(Pulido et al., 2019)
14	BD 2017	Jul 2017	Bangladesh	Nile tilapia	MN939372.1	(Chaput et al., 2020)
15	BD-2017-181	2017	Bangladesh	Nile tilapia	MT466437.1	(Debnath et al., 2020)
16	BD-2019E1	2019	Bangladesh	Nile tilapia	MT466447.1	(Debnath et al., 2020)
17	BD-2019-E3	2019	Bangladesh	Nile tilapia	MT466457.1	(Debnath et al., 2020)
18	USA-2019- WVL19054	2019	USA	Nile tilapia	MN193523-1	(Al-Hussinee et al., 2018)
19	USA-2019- WVL19031	Nov 2018	USA	Nile tilapia	MN193513.1	(Al-Hussinee et al., 2018)

727

728 Abbreviations: BC, barcode from Nanopore barcoding kit; country codes: TH, Thailand; IL, Israel; EC,
729 Ecuador; PE, Peru; and BD, Bangladesh. Animal codes: RT, red tilapia (*Oreochromis* spp.); NT, Nile tilapia
730 (*Oreochromis niloticus*); HT, hybrid tilapia (*Oreochromis niloticus* x *Oreochromis aureus*). Note that samples
731 No.3 and No.4 originated from the same fish specimens used to generate NCBI Sanger references TH-2018-N
732 (No. 11) and PE-2018_F3-4 (No. 13), respectively.
733

734 **TABLE 2** BlastN results of (A) 577 bp consensus sequences generated from the first round
735 PCR products; (B) 231 bp consensus sequences generated from the second semi-nested round
736 PCR products

737 (A)

Barcode samples	[†] Query length (bp)	NCBI top BlastN Hit TiLV isolate / accession number	% Identity
BC01	577	TH-2018-N / MN687745.1	100 (577/577 bp)
BC02	577	BD-2017-181 / MT466437.1	99.83 (575/576 bp)
BC03 [‡]	577	TH-2018-N / MN687745.1	100 (577/577 bp)
BC04 [‡]	577	PE-2018-F3-4 / MK425010.1	100 (577/577 bp)
BC05	577	PE-2018-F3-4 / MK425010.1	99.83 (576/577 bp)

738

739 (B)

Barcode samples	[†] Query length (bp)	NCBI top BlastN Hit TiLV isolate / accession number	% Identity
BC01	231	TH-2018-N / MN687745.1	100 (231/231 bp)
BC02	231	BD-2017-181 / MT466437.1	100 (230/230 bp)
BC03 [‡]	231	TH-2018-N / MN687745.1	100 (231/231 bp)
BC04 [‡]	231	PE-2018-F3-4 / MK425010.1	100 (230/230 bp)
BC05	231	PE-2018-F3-4 / MK425010.1	100 (230/230 bp)

740

741 [†] Query length of medaka consensus sequences with the primer-binding sites trimmed; [‡] Samples previously
742 Sanger sequenced; BC, barcode. For (B) note that for all samples, the BlastN results of consensus sequences
743 (231 bp) generated from sub-sampling (1k, 500, 100, 50 reads) were the same as the ones from no-subsampling.
744

745 FIGURES LEGENDS

746

747 **FIGURE 1** Overall workflow from sample collection of diseased fish on farm to sequence
748 results. The entire process takes less than 12 h. * DNA repair, end-preparation, multiplex
749 native barcode and adapter ligation
750

751 **FIGURE 2** (A and B) Identification of single nucleotide polymorphisms (SNPs) using
752 sequences alignment of TiLV segment 1 medaka consensus sequences (this study) with their
753 closest Sanger verified references. (A) Bangladeshi BC02 consensus (576 bp) aligned with
754 BD-2017-181 (MT466437.1) showing SNP in position 334 (red arrow); (B) Peruvian BC05
755 consensus (577 bp) aligned with PE-2018-F3-4 (MK425010.1) with SNP in position 347
756 (green arrow); (C and D) SNPs examination in Integrative Genomics Viewer (IGV) (version
757 2.8.10); (C) Read depth (BC02.medaka.bam file) aligned with final medaka consensus
758 sequence (BC02.medaka.fasta file) showing the SNP is partitioned between 274 and 620 bp
759 amplicons; (D) Read depth (BC05.medaka.bam file) aligned with final medaka consensus
760 sequence (BC05.medaka.fasta file) confirming the SNP is real since it is identical in 97% of
761 the reads, except for 1 homopolymer base-call error: G

762
763

764 **FIGURE 3** Maximum likelihood trees constructed in IQ-TREE based on the nucleotide
765 consensus sequences alignment of short TiLV consensus (577 bp and 231 bp) with TiLV
766 segment 1 reference sequences retrieved from GenBank database (Table 1). (A) Five 577 bp
767 consensus sequences compared with 14 reference sequences trimmed to 577 bp. (B) five 577
768 bp consensus sequences trimmed to 231 bp, five original 231 bp consensus sequences
769 compared with 14 reference sequences trimmed to 231 bp. The branch lengths indicate the
770 number of substitutions per site, and node labels indicate bootstrap support values in
771 percentage. Trees rooted using the mid-point rooting method

772

773 APPENDICES

774 Supplementary tables legends

775

776 **TABLE S1** NanoStat summary statistics of analysis of mixed amplicons (620 and 274 bp) for
777 each sample (BC01-05) using the full set of reads without sub-sampling. [†]Coverage or read
778 depth after clustering and filtering steps; [‡] mean percent identity of Nanopore raw reads to
779 each sample specific reference; [§] during basecalling; BC, barcode

780 **TABLE S2** NanoStat summary statistics of analysis of 274 bp amplicons for each sample
781 (barcode01-05) using the full set of reads and with sub-sampling (sub1K (1000), 500, 100, or
782 50 reads). [†]Coverage or read depth after clustering and filtering steps; [‡] mean percent identity
783 of Nanopore raw reads to each sample specific reference; [§] during basecalling; BC, barcode

784 Supplementary Figures legends

785

786 **FIGURE S1** Original 1% agarose gels showing detection of partial TiLV segment 1 from
787 five samples used in this study: (1) BC01, Thailand; (2) BC02, Bangladesh; (3) BC03,
788 Thailand; (4) BC04, Peru; (5) BC05, Peru; other samples (a to i) were not included in this
789 study. Gels were stained with ethidium bromide solution. M, 2-Log DNA marker (New
790 England Biolabs); Ng, negative control. Expected band size of 620 bp and 274 bp represent
791 amplicons from first round PCR and second round semi-nested PCR, respectively, with lanes
792 marked +++ for heavy infection, ++ for medium infection and + for a light infection. The
793 band marked with # on the right side of gels arose from cross hybridization of the amplified
794 products

795

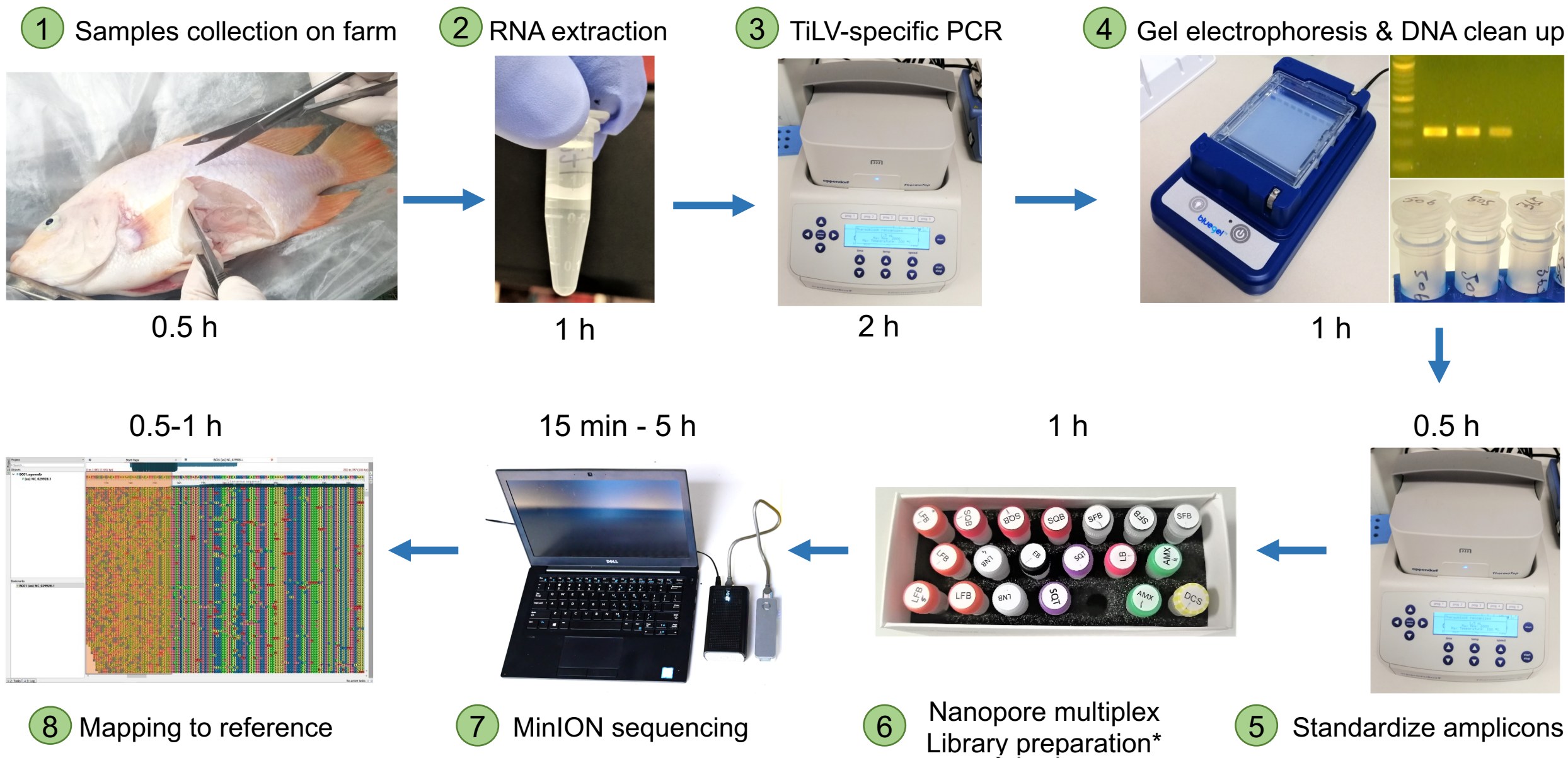
796 **FIGURE S2** Histograms of sample read counts generated every 5 min for 6 h. (A) BC01; (B)
797 BC02; (C) BC03; (D) BC04; (E) BC05

798

799 **FIGURE S3** Distribution of sequence lengths over all sequences between 50-1399 bp from
800 the mixed amplicons analysis (620 and 274 bp). (A) BC01; (B) BC02; (C) BC03; (D) BC04;
801 (E) BC05. Blue arrows indicate the peaks for 274 bp amplicons and green arrows the peaks
802 for 620 bp amplicons. Sequence length distribution obtained in FastQC High Throughput
803 Sequence QC Report (v 0.11.9) using final medaka.bam file as inputs. Figure produced in
804 GraphPad Prism 9.0.2; bp, base-pair

805

806



A

BC02	GCGCAGAAAATGCGTTCTCGTCAAAGACACTCTAGTAGAGTGTCCAGGAGGTATGTTGATGGGAATGTTAACGCAACTGCCACCTTGGCA
BD-2017-181	GCGCAGAAAATGCGTTCTCGTCAAAGACACTCTAGTAGAGTGTCCAGGAGGTATGTTGATGGGAATGTTAACGCAACTGCCACCTTGGCA
BC02	TTGCAAGGGACGACTGACAGATTCCGTCTTCAGCGATGACTTATAACATCGTTAECTCGCCCTGCTGAATTGCGCAGATAAGAGGACC
BD-2017-181	TTGCAAGGGACGACTGACAGATTCCGTCTTCAGCGATGACTTATAACATCGTTAECTCGCCCTGCTGAATTGCGCAGATAAGAGGACC
BC02	TACTTTCTGTAAGCTGTCAACAATTGTCGCTAAAGAAGAGTTACATTTCACTGGAAATAAAACTCGTGTACCCCTCACTAGGGAA
BD-2017-181	TACTTTCTGTAAGCTGTCAACAATTGTCGCTAAAGAAGAGTTACATTTCACTGGAAATAAAACTCGTGTACCCCTCACTAGGGAA
BC02	CGGTGACCTAGGCCACAGGGTTAGGCTGTACTGCTGGTGTCCCCTCAGGGGGCCAC
BD-2017-181	CGGTGACCTAGGCCACAGGGTTAGGCTGTACTGCTGGTGTCCCCTCAGGGGGCCAC
BC02	GGCGCTTGTGACTCAGGAGTTATGCCATTCCACTCAGCAGAACGCTATTCAGATAAAGCAGCAGGAATGTGCCCTATAGGTATAACCAACC
BD-2017-181	GGCGCTTGTGACTCAGGAGTTATGCCATTCCACTCAGCAGAACGCTATTCAGATAAAGCAGCAGGAATGTGCCCTATAGGTATAACCAACC
BC02	CCACTTACACAACGAGGAATGAGGACTTCTCTCCCCACATGCCCTGGGAGGGAGGACTGTAGTTAGCTTCAATCTCTACTGACTTTGGGACTG
BD-2017-181	CCACTTACACAACGAGGAATGAGGACTTCTCTCCCCACATGCCCTGGGAGGGAGGACTGTAGTTAGCTTCAATCTCTACTGACTTTGGGACTG
BC02	CCACCCATTGGTACCAAGTGCACCCCTGA
BD-2017-181	CCACCCATTGGTACCAAGTGCACCCCTGA

B

	10	20	30	40	50	60	70	80	90
BC05	GC	GC	AG	GA	AG	TT	CA	AC	GC
PE-2018-F3-4	GC	GC	AG	GA	AG	TT	CA	AC	GC
	100	110	120	130	140	150	160	170	180
BC05	CT	GC	AA	GG	AC	GA	CT	CG	CC
PE-2018-F3-4	CT	GC	AA	GG	AC	GA	CT	CG	CC
	190	200	210	220	230	240	250	260	270
BC05	TG	CT	TC	GA	AG	CT	GT	TA	CC
PE-2018-F3-4	TG	CT	TC	GA	AG	CT	GT	TA	CC
	280	290	300	310	320	330	340	350	360
BC05	CG	GT	AC	CT	AG	CC	AC	AG	CT
PE-2018-F3-4	CG	GT	AC	CT	AG	CC	AC	AG	CT
	370	380	390	400	410	420	430	440	450
BC05	GG	GC	GT	TT	G	AC	TC	AT	AG
PE-2018-F3-4	GG	GC	GT	TT	G	AC	TC	AT	AG
	460	470	480	490	500	510	520	530	540
BC05	CC	ACT	TAC	ACA	AC	GG	AA	GT	GG
PE-2018-F3-4	CC	ACT	TAC	ACA	AC	GG	AA	GT	GG
	550	560	570						
BC05	TC	AC	CC	AT	TT	CG	TA	CC	AC
PE-2018-F3-4	TC	AC	CC	AT	TT	CG	TA	CC	AC

BC02.medaka.
fasta

BCJz.medaka
.bam

330 bp 334 bp 338 bp

T T G T A A C T C

The diagram illustrates a DNA sequence across 15 horizontal lines. Key features include:

- Top Left:** A black bar labeled "4" is positioned above the first two lines.
- Top Center:** Two green "A" labels are placed above the third and fourth lines.
- Second Column:** A black bar labeled "2" is above the first line, and a black bar labeled "3" is above the second line.
- Third Column:** A green "C" label is above the third line, and a green "A" label is above the fourth line.
- Fourth Column:** A green "A" label is above the fifth line, and a green "A" label is above the sixth line.
- Fifth Column:** A green "A" label is above the seventh line, and a green "A" label is above the eighth line.
- Sixth Column:** A green "A" label is above the ninth line, and a green "A" label is above the tenth line.
- Seventh Column:** A green "A" label is above the eleventh line, and a green "A" label is above the twelfth line.
- Eighth Column:** A green "A" label is above the thirteenth line.
- Ninth Column:** An orange "G" label is above the fourteenth line, and an orange "G" label is above the fifteenth line.
- Bottom Right:** A black bar labeled "2" is positioned below the fifteenth line.

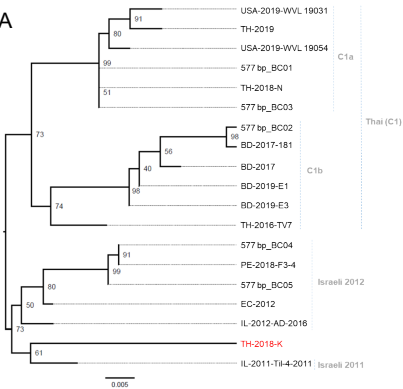
D

343 bp 347 bp 351 bp

A C A G A C T G C

3BC05.medaka.

A



B

